

## MD simulations of Ag film growth using the Lennard-Jones potential

This article has been downloaded from IOPscience. Please scroll down to see the full text article.

1996 J. Phys.: Condens. Matter 8 8753

(<http://iopscience.iop.org/0953-8984/8/45/011>)

View [the table of contents for this issue](#), or go to the [journal homepage](#) for more

Download details:

IP Address: 171.66.16.207

The article was downloaded on 14/05/2010 at 04:27

Please note that [terms and conditions apply](#).

# MD simulations of Ag film growth using the Lennard-Jones potential

P Guan, D R McKenzie and B A Pailthorpe

School of Physics, University of Sydney, Broadway, NSW 2006, Australia

Received 10 May 1996, in final form 16 July 1996

**Abstract.** The nucleation and growth of Ag films on a Cu(100) substrate were studied by molecular dynamics simulation using Lennard-Jones (L-J) interactions. Different mechanisms were found for island formation on low- and high-temperature substrates. Improved agreement between the simulation and experimental LEED patterns was obtained when the L-J interaction was modified to take into account the location of the atoms on the surface or in the bulk. The simulation predicted a  $c(2 \times 10)$  unit mesh and low surface roughness, as was observed experimentally. The L-J interaction gives three-dimensional growth, but can be made to reproduce the observed layer by layer growth if the force constant for surface atoms is further modified.

## 1. Introduction

The subject of thin film growth by molecular-beam epitaxy (MBE) has proved over the past decade to be an interesting subject for fundamental studies as well as for device applications. The understanding of growth mechanisms is of importance in the prediction of material properties and for device fabrication using interface-dominated structures like superlattices and metal–semiconductor junctions.

Although experimental techniques, such as low-energy electron diffraction (LEED), Auger electron spectroscopy and electron microscopy can be used to determine structural properties like the registration of adatoms on the substrate and the three-dimensional growth mode, it is still difficult to obtain experimental information on the dynamical aspects of film growth on the atomic scale. The purpose of the present paper is to reproduce experimental observations and to study detailed dynamical behaviour using computer-generated structures.

In metals, the interactions are essentially many-body in nature. The modelling of many-body interactions is possible using quantum mechanical techniques based on density functional theory, but the demands on computational resources are too great at the present time to allow large systems to be studied with full dynamics, as is necessary to study the growth of surface layers. Schemes which approximate the quantum theory with a type of effective medium theory are attractive computationally. One approach is the ‘embedded atom method’ [1], which derives interaction parameters from density functional theory. In this paper we prefer to use the Lennard-Jones potential as a starting point because of its computational convenience and its widespread use in modelling interactions in metals. The approach adopted here is to modify the energy parameter  $\epsilon$  so that the reduced interaction energy resulting from the lower coordination of surface atoms is accounted for. The validity

of this approach has already been demonstrated by the modelling of the surface phonons in metals [2–5].

We will apply our method to the growth of Ag on Cu(001) with the aim of reproducing experimental observations and studying the detailed dynamics of the film growth process. Previous simulations of film growth using the L-J potential concentrated only on the dependence on the size-mismatch of the two different atoms in the structure. We will use two different  $\varepsilon$  values, one for the bulk environment and the other for the surface environment. The influence on the deposited layer structure from the parameter  $\varepsilon$  is only noticeable for certain mismatches, as discussed in [6] and it turns out that the Ag/Cu(001) system lies in the range within which these effects should occur. The Ag/Cu(001) system is therefore a good choice for study.

An intriguing feature of experimental observations of some metal FCC layers deposited on the (100) surface of several FCC metals is the formation of portions of the hexagonal close-packed structure. A detailed study of LEED patterns shows that the structure is commensurate with the substrate in one direction and almost incommensurate in the other direction, forming a unit cell extended in one direction. For example, a monolayer of silver forming  $c(2 \times 8)$  cells occurs on Ni(100) substrates, whereas  $c(2 \times 10)$  cells are formed on Cu(100) substrates. Gold, on the other hand, forms  $c(2 \times 14)$  unit cells on Cu(100) substrates. In our simulation of Ag on Cu(001), an overlayer  $c(2 \times 10)$  pattern was obtained. To obtain more insight into this MBE process, simulations on the dynamics of Ag island nucleation on Cu(100) surfaces were also performed.

## 2. Background

Direct simulation of the kinetic processes occurring on an atomic scale during MBE growth for systems containing a sufficiently large number of atoms to obtain a realistic description of the process has only recently become possible. With the development of fast computers and the application of the molecular dynamics technique, Rahman's group [7] performed the first such simulation using a Lennard-Jones potential of growth on the (111) faces of a FCC lattice. The incident beam atoms were of the same kind as the substrate atoms and produced a well-ordered overlayer. They then studied a mixed incident beam consisting of two kinds of incident atoms with the same cohesive energy, but different atomic radii, one of which was the same as that of the substrate atom. Amorphous overlayers were formed once the difference in the atomic radii exceeded a critical value of 10% [8]. Following this, Paik and Das Sarma [9] extended the investigation to the MBE process for growth on various orientations of a FCC substrate using a Lennard-Jones model. Their results show that films grown from different directions have different degrees of perfection: the [111] direction has the lowest incidence of defects and the [110] direction has the highest.

Hara *et al* [6] performed a systematic study of hetero-epitaxial MBE on the (001) surface of FCC structures. They studied the growth pattern of the first few overlayers using a two-component L-J system such that the atomic size of the incident beam is different from that of the substrate but still has the same cohesive energy. The overlayer structure was found to depend on the degree of mismatch in atom sizes: with increasing mismatch between the incident beam and the substrate, three different patterns of overlayer structure were formed. These were  $c(1 \times 1)$ , triangle and  $\sqrt{2} \times \sqrt{2} - R45^\circ$ . Aubin *et al* [10] performed a MD simulation of superlattice growth using a similar treatment. To date, simulations performed with Lennard-Jones potentials have not been adapted to particular systems and important experimental observations have not been reproduced. An example is the growth mode. The growth modes of relevance here are the Volmer–Weber (V–W) and

Stranski–Krastanov (S–K) ones. The V–W mode is an island-type growth mode in which the second overlayer growth begins before the first monolayer is complete, producing a three-dimensional structure. In S–K growth, the onset of the second layer occurs after the first layer has completely formed, and subsequent growth occurs via nucleation and coalescence of 3D islands. All the simulations above showed a three-dimensional V–W growth mode [6–10] from the start of the film growth, which is not true in practice. The results in this paper prove that the V–W growth mode results from inadequacies in the model itself rather than from the properties of the system studied. More realistic embedded-atom-method (EAM) potentials have recently been employed successfully to model the bilayer growth of Au on Ni(100), Ni on Au(100) [11] and Ag on Ag(111) [12]. It is interesting to note that, using the EAM method, the Au growth on Ni(100) exhibits a S–K [11] (three-dimensional growth following initial two-dimensional growth) growth mode which is not observed with the L–J models. Yang *et al* [13] investigated the difference between the pair potential and the EAM method in detail by performing a MD simulation of Ag growth on Ni(100) using both models. Their results show that there is a qualitative agreement between these two models at room temperature when displacements of atoms are small. We adopt the viewpoint in this paper that pair potentials can be used to describe the surface and interface properties if parameterized properly at room temperature.

### 3. Computational details

The Cu(001) substrate consists of ten layers which were grouped into three types depending on the nature of the boundary conditions. The bottom two layers were fixed. The next two layers were used as a thermal bath to remove the deposited energy from the system so that the temperature of the system did not rise uncontrollably. The remaining six layers were free to move and comprised the substrate upon which film growth was performed. There were 160 atoms in each layer.  $x$  and  $y$  axes were chosen parallel to the cubic unit cell edges within the substrate layer. The  $z$  axis is in the direction normal to the substrate. Periodic boundary conditions were applied in the  $x$  and  $y$  directions. The incident atoms had 0.2 eV kinetic energy, which is suitable for the case of evaporative deposition, and were introduced randomly at a normal direction every 300 time steps. One time step is 0.0018 ps. The atoms interacted via the Lennard-Jones potentials

$$U(r) = 4\varepsilon \left[ \left( \frac{\sigma}{r} \right)^{12} - \left( \frac{\sigma}{r} \right)^6 \right] \quad (1)$$

where  $\varepsilon$  is the bond energy and  $\sigma$  measures the atomic size. For a two-component system, as studied here, the parameters for the mixed interaction between these two types of atoms can be estimated by the simple average suggested by Steel *et al* [14]:

$$\varepsilon = (\varepsilon_a \varepsilon_s)^{1/2} \quad \sigma = \left( \frac{\sigma_s + \sigma_a}{2} \right)$$

where  $s$  and  $a$  represent substrate and adatoms respectively. In our simulation, these parameters were taken from [15] and are given in table 1.

The lattice mismatch between the two elements is 13%. For ease of calculation, we used equation (1) and the parameters in table 1 for the idealized, bulk model (model B hereafter) study since they had been obtained by fitting to bulk crystalline properties. During the film growth, new Ag atoms are introduced as surface atoms and later, as more atoms are introduced, these early atoms will be buried by newly arriving atoms and so become bulk atoms. Since the coordination of surface atoms is different from that of bulk atoms, the

**Table 1.** Parameters for the L-J potentials in the study.

	$\varepsilon$ (eV)	$\sigma$ (Å)
Cu	0.4096	2.338
Ag	0.3450	2.644

strength of interaction between surface atoms is less than that between bulk atoms. This effect has been observed [2–5] using surface-phonon dispersion. For Ag, lattice dynamics slab calculations have been performed with pair potentials by Bortolani *et al* [3]. The result showed that the anomalous phonon branches of surface modes could be reproduced by softening the in-plane surface force constant by half. A similar result was also obtained for Ni thin films grown on Cu(100) with a pair potential [2]. Many-body potentials have also been used to explain surface-phonon anomalies in Ag [4, 5]. On the other hand, more recent calculations using many-body interactions have explained the surface-phonon softening with a quite modest reduction in the surface force constant compared with the pair-potential model. However, because we have used the pair-potential model in this study, to be consistent with Bortolani *et al* we need to adopt a surface energy parameter which is half that applying to the bulk, namely  $\varepsilon'_a = 0.5\varepsilon_a$  in our model. This surface model we will refer to as the S model. In the simulation, we switch from the surface potential to the bulk potential when those atoms initially on the surface become bulk atoms. For simplicity, this switch was activated layer by layer; whenever a layer had been covered fully by its upper layers, we changed its potential from  $\varepsilon'_a$  to  $\varepsilon_a$ . The simulation used the standard Verlet algorithm [16]. In simulations using either the S or the B model, the interactions were extended to second-nearest-neighbour atoms. The substrate was thermostatted to 300 K before the introduction of the adatoms.

## 4. Results and discussion

### 4.1. The dynamics of nucleation

To understand how the hexagonal overlayer was formed on the Cu(100) substrate, 100 Ag atoms were deposited onto substrates held at 300 and 80 K respectively. Here only the S model was used. The results show that the pattern of the adatom arrangement was dependent on the temperature. Figure 1 shows the arrangement of adatoms on the two substrates for the same number of atoms deposited. At low temperature, some atoms form a close-packed structure which is not visible at higher temperature (see figure 1). For a quantitative description of the structure, the radial distribution function  $G(r)$  of these Ag atoms is plotted in figure 2 for the two circumstances.  $G(r)$  is defined by  $G(r) = 4\pi r(\rho(r) - \rho_0)$ , where  $\rho_0$  is the average density of the structure and  $\rho(r)$  is the density of atom centres at a distance  $r$  from an atom. We can see that the first peak is much higher at low temperature than it is at high temperature, which indicates that there are more close-packed patterns in the low-temperature case. Another difference was the tendency at low temperature for a second layer of growth to form at an earlier stage. On a low-temperature substrate, small and separately distributed hexagonal close-packed islands formed first and full coverage was eventually achieved by merging of these islands. On the other hand, at the higher temperature, the close-packed hexagonal structure does not form at low coverage. Most atoms fall into the hollows of the substrate until a close-packed hexagonal overlayer has eventually been formed.

To gain more insight into the formation of hexagonal islands on the low-temperature

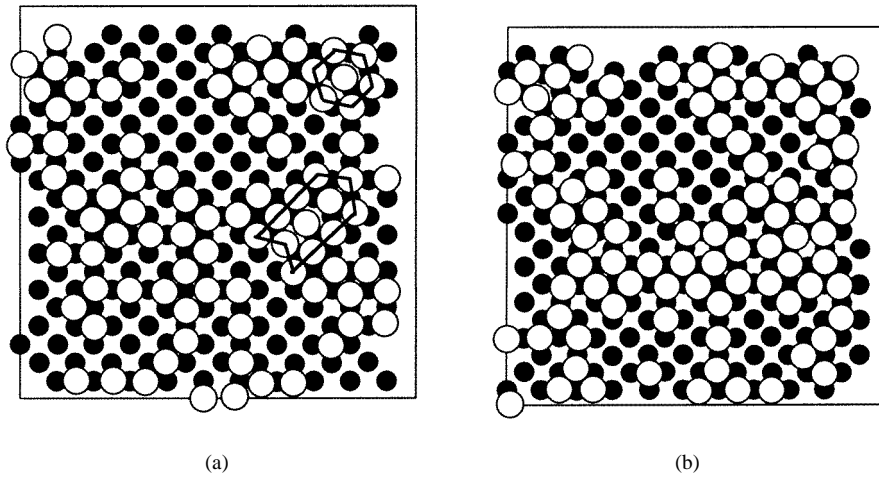


**Figure 1.** The configuration of adatoms after 100 atoms have been deposited on the Cu(100) at (a) 80 and (b) 300 K.

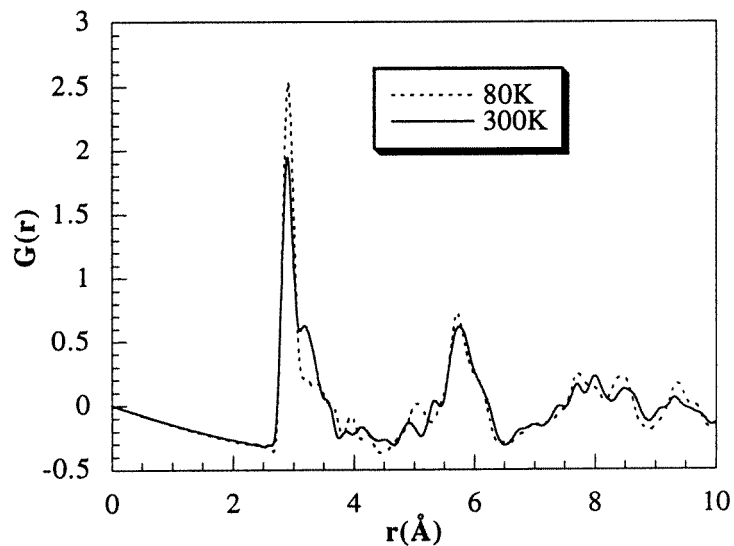


**Figure 2.** The distribution function for silver atoms on the Cu(100) surface.

substrate, small two-dimensional Ag clusters of up to eight atoms were grown in the central area of the substrate. The time interval between two deposited atoms was long enough for the former deposited Ag atoms to reach a stable state. We found that, for a cluster of less than seven atoms, the Ag atoms were located roughly at the hollow sites of the substrate surface, as shown in figures 3(a) and (b). In figure 3, two different sites A and B are identified. No features of the hexagonal structure appear at this stage. When another atom is deposited at the B site, the island evolves in 0.13 ps to the structure of figure 3(c) in which a pattern of the close-packed Ag(111) structure can be seen. Any attempt to add

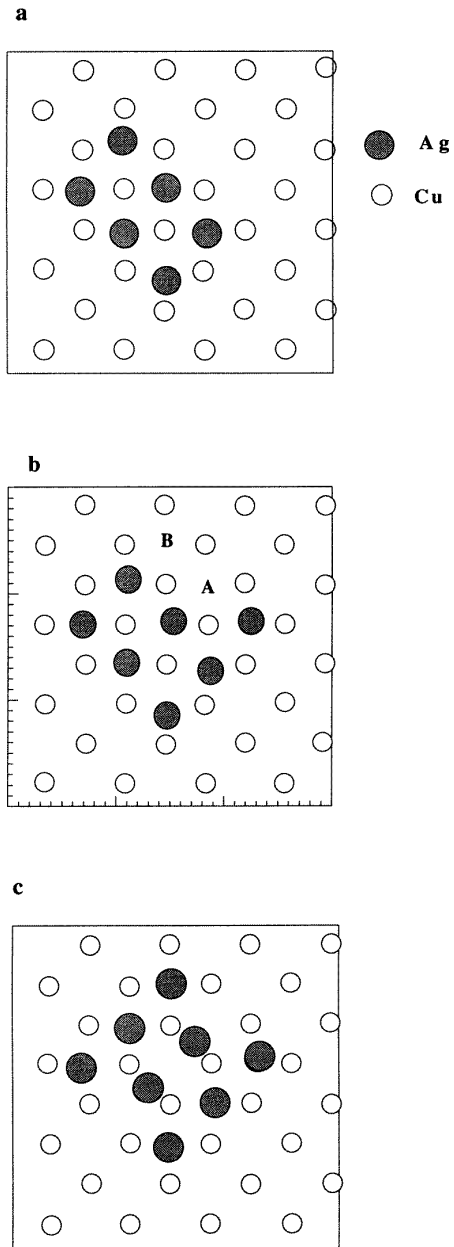


**Figure 3.** An illustration of how the close-packed pattern evolves with increasing number of atoms in a small Ag cluster.

an atom at the A site of figure 3(b) failed because the adatom either was pushed away or jumped to the B site.

#### 4.2. The growth mode

The S model produced more atoms filling the first monolayer. The layers of the grown film are defined by calculating its density profile along the  $z$  direction, which will be shown in

the next section. Figure 4 shows the numbers of deposited atoms in the first and second layers as functions of the total number of atoms deposited using the two models (S and B models). We see that, in both cases, the film growth demonstrates a characteristic V–W growth mode. In common with previous L–J results [6–9], we found no other type of growth mode. Since non-island growth is observed experimentally for the Ag–Cu system [17, 18], in which deposition of one monolayer of Ag on a Cu(100) surface was achieved, it appears that the L–J potential is not sufficiently realistic to predict the growth mode. Further evidence for this conclusion is obtained from Luedtke and Landman [11] calculation using the EAM model, whereby a S–K growth mode was obtained for Au growing on Ni(100). The L–J model does not correctly describe all the processes occurring when the adatoms approach descending steps from the upper terrace.

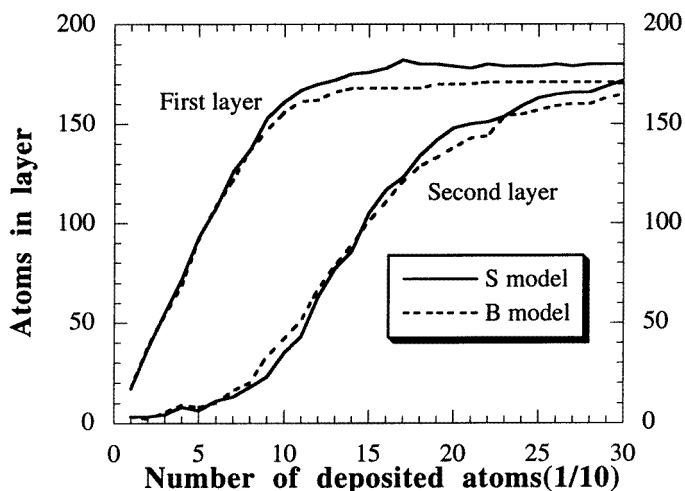


**Figure 4.** The number of atoms in the first two layers of the film as a function of the number of atoms deposited.

Two mechanisms are available for second-layer atoms to descend to the first monolayer. These are movement of a second-layer atom over the edge of the island region and the descending of the atom into the first monolayer at an interior point in the island [19]. The EAM model allows the second of these mechanisms to occur [20] and so layer by layer growth results. The L–J potential did not allow this process to occur in any of the simulations we performed and atoms only entered the first layer by the first of these mechanisms. Tests were performed by further reducing the force constants of the adatoms in the S model to 25% of their bulk value. In that case a descending of the adatom on the upper layer to the first layer with the second mechanism occurred, as shown in figure 5. The embedded atom method gives much more realistic potentials which automatically include the effect of the weaker surface bonds and the effect of three-body interactions which are important in the energetics of the second process described above.

In our simulations, the S model gave a greater degree of descending to the lower layers, probably because the barrier at the edge of the island is not as high as that in the B model. It should be noted that the structure of the first monolayer is dependent on the value of  $\epsilon$  in the L–J potential. In a study of structure as a function of mismatch, Hara *et al* [6] found that, at the 13% mismatch which applies to our Ag–Cu system, a structure based on equilateral



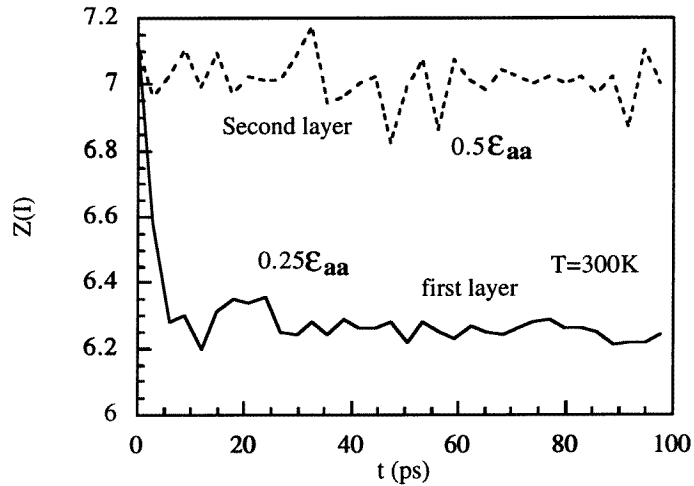


**Figure 5.** A further reduction in force constant resulting in the adatoms descending to the first layer with the second mechanism.

triangles was formed rather than the  $c(2 \times 10)$  structure. We ascribe the difference between our results and those of Hara *et al* to a smaller value of  $\varepsilon$  in the L-J potential.

Figure 6 shows the structure of the first monolayers for the S model. We can see that the overlayer atoms exhibit a periodic coincidence with the substrate atoms. This agrees well with the experiment results using LEED, which show that Ag atoms formed a  $(2 \times 10)$  unit mesh on Cu(100) [18]. The B model yielded a  $c(2 \times 8)$  unit mesh. In the simulation, the structure transition of the first overlayer as in the Au–Ni case [11] was not observed, perhaps because of the over-simplified method we used in modelling the potential variations, namely layer by layer switching of two different model potentials during the film growth.

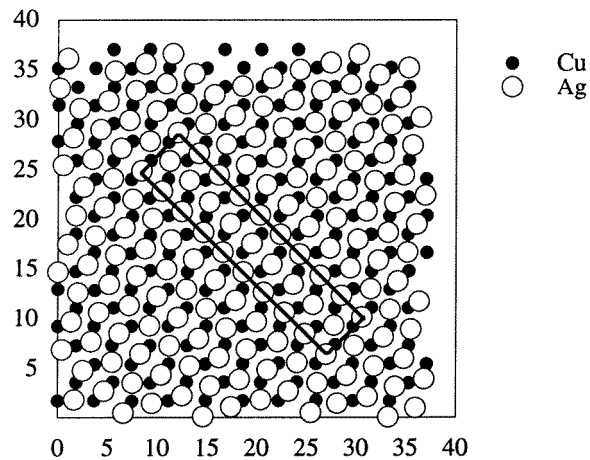


**Figure 6.** The atomic arrangement in the first Ag monolayer on Cu(100). The  $c(2 \times 10)$  cell is shown.

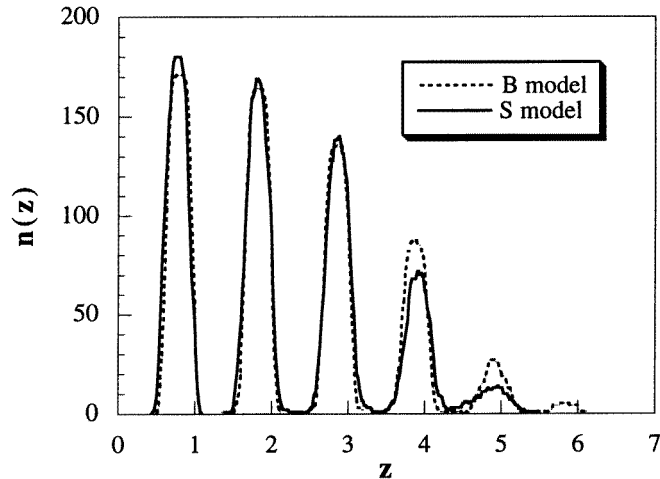


**Figure 7.** The number density along the  $z$  axis of the 598 atom Ag films for the S and B models.

Comparing with the interatomic distance of the Ag bulk crystal, we found that the  $(2 \times 10)$  mesh is achieved through 1.694% compression in the Cu[110] direction and approximately 2.06% expansion in the Cu[110] direction. These distortions agree well with experimental measured values of 1.7 and 2% [18]. The compressive stress in the [110] direction may cause corrugation of the Ag line and could possibly be relieved by ejecting atoms to the upper layer under an unbalanced compression from the upper layers, a process seen by other authors in the Au–Ni system [11]. In our simplified model, however, this ejection process was not observed.

#### 4.3. Surface roughness induced during the film growth

Figure 7 shows the number density for the two films of 598 atoms generated by the two (S & B) models along the  $z$  axis. It is apparent from figure 6 that, for the same number of deposited atoms, films grown with the S model have a tendency for atoms to shift to the lower layers compared with those grown with the B model for the reasons discussed in section 4.2. It can also be seen from the surface topography that the film grown with the S model has a smoother surface. The film obtained by the B model contained some deep valleys. If we denote the peak to peak roughness of the surface by the number of layers between the bottom of the valley and the top of the high points, the roughnesses for these two films are 3 and 5 respectively.

## 5. Conclusion

In this study of simulation of growth using L-J potentials, we have found several parameters which affect the type of growth. For Ag on Cu(100), growth at high temperature causes the hexagonal close-packed structure to disappear at low coverage. The L-J potential has limitations in that it always gives V–W growth and does not allow atoms from the second layer to enter the first layer by the exchange mechanism. The use of a modified L-J potential (a factor of two reduction in the force constant) for surface atoms gives better agreement

with more sophisticated models such as the EAM model and gives a closer approach to layer by layer growth, albeit without fully achieving it. A further reduction in the force constant for surface atoms by a factor of two does show a tendency towards layer by layer growth. The strength parameter  $\varepsilon$  is therefore very important and its value affects the structure of the grown layers.

### Acknowledgments

The authors acknowledge financial support by Overseas Postgraduate Research Scholarship and University Postgraduate Research Awards within Sydney University. We wish to thank VisLab at the University of Sydney for access to the Cray supercomputer and extensive visualization resources. Special thanks are due to N A Marks for his help throughout the research.

### References

- [1] Daw M S and Baskes M I 1984 *Phys. Rev. B* **29** 6443
- [2] Stuhlmann C and Ibach H 1989 *Surf. Sci.* **219** 117–27
- [3] Bortolani V et al 1984 *Phys. Rev. Lett.* **52** 429
- [4] Jayanthi C S et al 1987 *Phys. Rev. Lett.* **59** 795
- [5] Kaden C et al 1992 *Phys. Rev. B* **46** 13509
- [6] Hara K et al 1989 *Phys. Rev. B* **39** 9476
- [7] Schneider M, Rahman A and Schuller I K 1985 *Phys. Rev. Lett.* **5** 604
- [8] Schneider M, Rahman A and Schuller I K 1986 *Phys. Rev. B* **34** 1802
- [9] Paik S M and Das Sarma S 1989 *Phys. Rev. B* **39** 1224
- [10] Aubin E and Lewis L J 1993 *Phys. Rev. B* **47** 6780
- [11] Luedtke W D and Landman U 1991 *Phys. Rev. B* **44** 5970
- [12] Gilmore C M and Sprague J A 1991 *Phys. Rev. B* **44** 8950
- [13] Yang L and Rahman T S 1992 *Surf. Sci.* **278** 407–13
- [14] Steel H A 1974 *The Introduction of Gases with Solid Surfaces* (Oxford: Pergamon)
- [15] Halicioglu T and Pound G M 1975 *Phys. Status Solidi a* **30** 619
- [16] Verlet L 1967 *Phys. Rev.* **159** 98
- [17] Bauer E 1967 *Surf. Sci.* **7** 351
- [18] Palmberg P W and Rhodin T N 1968 *J. Chem. Phys.* **49** 134
- [19] Kellogg G L 1944 *Surf. Sci. Rep.* **21** 48
- [20] Luedtke W D and Landman U 1994 *Phys. Rev. Lett.* **73** 569